

A 3D Smooth Random Walk Mobility

Model for FANETs

Na Lin¹, Feng Gao¹, Liang Zhao¹, Ahmed Al-Dubai², Zhiyuan Tan²

¹*School of Computer Science, Shenyang Aerospace University, Shenyang, China*

²*School of Computing, Edinburgh Napier University, UK*

Abstract— The number of Unmanned Aerial Vehicles (UAVs) applications has increased over the past few years. Among all scenarios, UAV group consisting multi-UAVs is normally used to provide extensible communications. As a networking solution, Flying Ad Hoc Networks (FANETs) routing with ideal routing performance is the prerequisite of the multi-UAV application. Regarding the high construction cost of devices for FANETs, it is infeasible to build the real experimental environment, hundreds of UAVs are needed. In this case, network simulation is the most common mean to study FANETs in most cases. For FANETs, the mobility of UAV nodes has an important impact on the simulation results. Thus, a mobility model which can fit into specific environments well is necessary. Traditional mobility models of FANETs are mainly designed for planar scenarios without considering the actual application of FANETs which is three-dimensional (3D). Therefore, in this paper, firstly, the characteristics of UAVs is analyzed and then the key points of 3D mobility model for FANETs are presented. In this context, we propose a 3D Smooth Random Walk (3DSRW) mobility model, which intends to mimic the mobility of UAVs to the greatest extent. Then, we conduct simulations to get the network performance of AODV to verify the performance gap between 2D and 3D environment, in order to demonstrate the validity of our proposal. To further present the usage of our proposal, we show the performance of four routing protocols, including AODV, DSDV, OLSR and GPSR under the 3DSRW-constructed 3D environment, and analyzed their applicability in 3D environment.

Keywords—Flying Ad Hoc Networks, FANETs Mobility Model, 3D FANETs Simulation, 3D, Smooth Random Walk, FANETs Routing Protocols

I. INTRODUCTION

Nowadays, UAVs have been popularized in all aspects of people's lives, including military applications and civilian applications. In the civilian sector, people deploys various sensors and network devices on the UAVs to detect and collect air and ground information on specific areas. In this context, UAV can be applied to monitor a certain traffic section, carry out rescue and search missions [1]. More, in logistic industry, UAVs has been also applied to solve the last-mile problem of express delivery. In military, because the UAV is smaller and faster, it can be applied for regional reconnaissance, remote sensing and monitoring, and joint combat operations.

Among the numerous studies on UAV, the research on UAV cooperative engagement, Air-To-Ground cooperative engagement and UAV cooperative delivery has shown the great significance [4]. There is a common feature of these applications: (1) a group of UAVs work together to accomplish complex tasks; (2) they form a group of drones, and collaborate. In this case, network communication is a vital to UAV collaboration. As a solution, FANETs (Flying Ad Hoc Network) [2] is designed as a special case of Mobile Ad

Hoc Networks (MANETs) where the FANETs has its characteristics as followings.

Moving area: the UAV free flight in three-dimensional space, which makes its network topology a three-dimensional structure rather than a planar structure (standard MANETs or vehicular networks).

Rapid movement: the flight speed of UAV is faster, which makes its network topology structure changes frequently.

Speed and turning angle limits: the speed is with certain limits; in addition, for the fixed-wing UAV, there is no emergency stop and sudden turning during the operation.

Energy supply: since the drone is flying in the air, its energy must be considered where we have to prevent UAV from crashing due to insufficient energy in the air.

Safety: UAVs flying in the air are vulnerable to physical obstacles, communication interruptions or human interception security threats.

Fig 1 shows an application scenario of FANETs. In case of congestion or sparse vehicle network, UAVs flying in the air can be used as relay nodes for data transfer to ensure data transmission between vehicles. These UAVs fly over the city to assist the ground vehicle network to form G-FANETs [3].

FANETs experiments in real-world environments are expensive to construct. In the study of FANETs, most of existing work adopts the simulation experiments, such as OMNET++, OPNET++, NS3, MATLAB and NS2 with

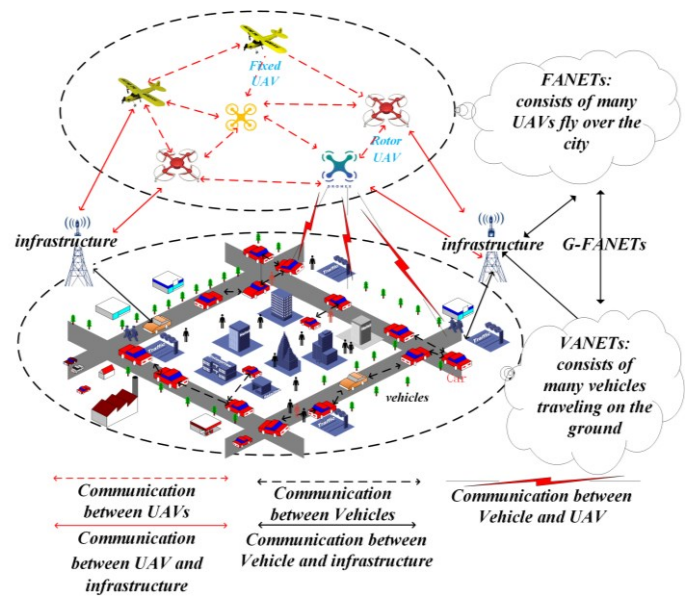


Fig. 1. G-FANETs Framework

mimicking the mobility and communication of the UAVs in a more realistic way, and evaluate the routing protocol under certain performance metrics.

Existing studies of routing protocols on FANETs most employ the mobility model of MANETs [5] to conduct experiments, where the mobility model include random walk, random way point, and gauss markov. Although applying these models is very straightforward, these two-dimensional models cannot provide the real movements of UAVs because the UAVs fly in three dimensions. [6] studied and proved that mobility models have effects in FANETs performances in simulations. When evaluating the performance of various types of FANETs routing protocols, a mobility model that can mimic the UAV's mobility characteristics to the greatest extent is critical to the experiment. Due to the vital impact of the mobility model on network performance, using the existing 2D ad-hoc mobility model may result in erroneous simulation results. In this paper, we propose a 3D Smooth Random Walk mobility model which could mimic the mobility of UAVs to the greatest extent. Then we use the mobility model to conduct simulations in many different scenarios.

In order to make the FANETs simulation more realistic simulation of the movement of the UAV, we comprehensively analyzed the mobile characteristics and mechanical characteristics of the UAV, and constructed a FANETs 3D smooth random walk mobility model. We list the following contributions of this work below.

- a) We propose a 3DSRW mobility model from the 3D speed processing, 3D boundary processing and 3D track smoothing of the UAV in the mobility model.
- b) We modify the existing simulation system NS2 to support both 2D and 3D simulations and systematize the proposed 3DSRW mobility model to be compatible with NS2.
- c) We experiment with the proposed 3DSRW mobility model and the modify simulation system. Compare the performance of various types of protocols in the 3D FANETs environment.

This paper is organized as follows. Section II introduces the related work, mainly including an overview of the ad-hoc mobility model and a detailed introduction of the random walk mobility model. In Section III, we propose 3D smooth random walk mobility model inspired by the random walk mobility model. In Section IV, the construction of simulation platform is introduced, then the parameter setting and the protocol used in the experiment are briefly introduced, and the proposed 3DSRW mobility model is applied to various simulation environments. Finally, we conclude this work.

II. RELATED WORK

We will depict several mobility models suitable for FANETs in 2D scenarios. Among them random walk mobility model is the most common one adopted by researchers where we will improve it afterwards. Thus, in this section, we discuss this model in more depth than the other models. Before presenting FANETs mobility models, we will introduce some classical mobility models of MANETs, including entity and group mobility models. The random walk and gauss markov mobility model in entity mobility model, and reference point group mobility model in group mobility model are presented.

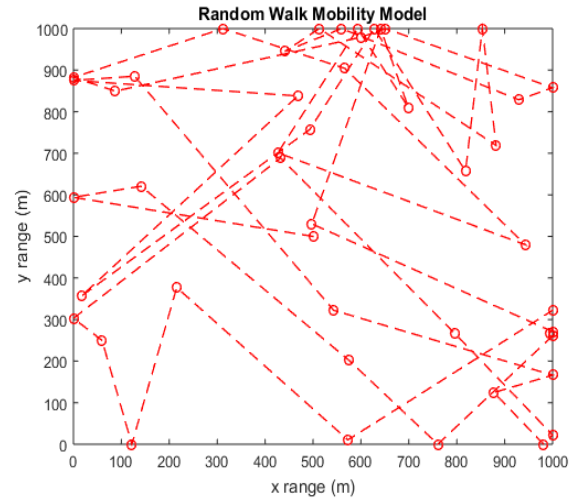


Fig. 2. Random Walk mobility model trace

Among the mobility models specially designed for FANETs, we choose the smooth turning and the particle swarm mobility model, which are the mainstream models for FANETs simulation at present.

A. Random Walk Mobility Model.

Random walk mobility model [7] is a classical model which inspired by individual entities in nature move in extremely unpredictable ways. Random walk model mimics these unstable movements. In this model, the node randomly generates an initial position in a specific area. When the node moves from its current position to a new position, the node randomly selects a direction D in pre-defined range of $[0, 2\pi]$, the velocity V in range of $[V_{\min}, V_{\max}]$ and constant travel time T or constant travel distance L . At the end of the travel time T or travel distance L , the node chooses a new direction and speed as before. When the moving node reaches the simulation boundary, the moving direction of the node is calculated according to the optical reflection mechanism. The Random Walk Mobility Model does not consider the turning angle problem in the direction selection and boundary processing. Especially for the fixed-wing UAV, the turning angle has strict limits, and the model is time-independent. That is, the speed and direction of the previous period will not affect the next moment, which does not meet the dynamic limit of the UAVs. Thus, we need to improve it to suit specific FANETs scenarios. The trace generated by random walk is shown as Fig 2.

B. Gauss Markov Mobility Model

The gauss markov mobility model [8] was originally proposed to simulate a personal communication system and was later applied to simulate a mobile ad hoc network. It is a time-dependent moving model, initially with a speed value and direction at a fixed time. The movement trajectory is generated by updating the velocity and the direction within the interval τ . The velocity S_n and the direction value D_n of the n^{th} period are based on the velocity $S_{(n-1)}$ and the direction value $D_{(n-1)}$ of the $(n-1)^{th}$ period. Equation(1) and (2) are the updating methods of velocity and direction of the model:

$$S_n = \alpha S_{n-1} + (1 - \alpha)\bar{S} + \sqrt{(1 - \alpha^2)}W_{n-1} \quad (1)$$

$$D_n = \alpha D_{n-1} + (1 - \alpha)\bar{D} + \sqrt{(1 - \alpha^2)}V_{n-1} \quad (2)$$

where S_n and D_n are the new velocity and direction values of the node in the period n , α is the memory factor in the range of $[0,1]$, and \bar{S} and \bar{D} are the mean values of the velocity and direction when $n \rightarrow \infty$, W_{n-1} and V_{n-1} is a random variable from Gaussian distribution. By adjusting the value of α , the effect of historical speed and direction on the next speed and direction is changed. Specially, when $\alpha = 1$, the speed and direction of the node in the next period are the same. The linear motion moves at a constant speed. When $\alpha = 0$, the nodes move randomly. The position of the next time period of the node is calculated by the current position, velocity and direction of the node, and the node position of the n^{th} time period is calculated by (3) and (4):

$$X_n = X_{n-1} + S_{n-1} \cos(D_{n-1}) \quad (3)$$

$$Y_n = Y_{n-1} + S_{n-1} \sin(D_{n-1}) \quad (4)$$

where (X_n, Y_n) and (X_{n-1}, Y_{n-1}) is the position of the node in the period n^{th} and the period $(n-1)^{th}$, S_{n-1} and D_{n-1} is the speed and direction of $(n-1)^{th}$ time periods. The Gauss Markov model uses the average direction method for boundary control. The model is temporal dependence. From the simulation trajectory, it can be seen that the sudden stop and sharp turn will not happen, which is more in line with the characteristics of UAV movement.

C. Reference Point Group Mobility Model

In Ad Hoc Network, mobile nodes often run in groups. For the emergence of UAV nodes, the group movement model is necessary. Here we introduce a classic group mobility model: Reference Point Group Mobility Model (RPGM) [9].

In this model, all nodes are divided into groups, each of which has a reference center, which can make a logical center point or a predefined reference node. The nodes in the group move along with the center point. The other nodes in the model center node group move according to the Random Way Point Mobility Model, and the mobile nodes cooperate with each other. The equation of the model is given in (5):

$$\vec{V}_i^t = \vec{V}_{group}^t + \overline{RM}_i^t \quad (5)$$

where \vec{V}_i^t represents the movement vector of the group member i at time t , \vec{V}_{group}^t represents the group movement vector at time t , and \overline{RM}_i^t is a random variable indicating the distance of the group member i from the center node of the group. \overline{RM}_i^t is a stochastic process of independent and identical distribution, the value of \overline{RM}_i^t is in the range of $[0, 2\pi]$. As the individual reference points move from time t to $t+1$, their locations are updated according to the group's logical center. Once the reference points are updated, the reference point of the group at time $t+1$ named $RP(t+1)$ is calculated. By choosing the appropriate center point and adjusting other parameters, the model can mimic a variety of mobile behaviors. The distance between the nodes in the group and the center node of the group is changed by adjusting the \overline{RM}_i^t parameter, so that no collision occurs between the nodes. The center node of group can also change the distance between groups by adjusting similar parameters. Since all nodes of the model use the Random Way Point Mobility Model, they will not move outside the simulation area, which avoids the boundary control problem well. However, the random waypoint model also has some problems, for example, the maximum corner problem. The trace generated by reference point group mobility model is shown as Fig 3.

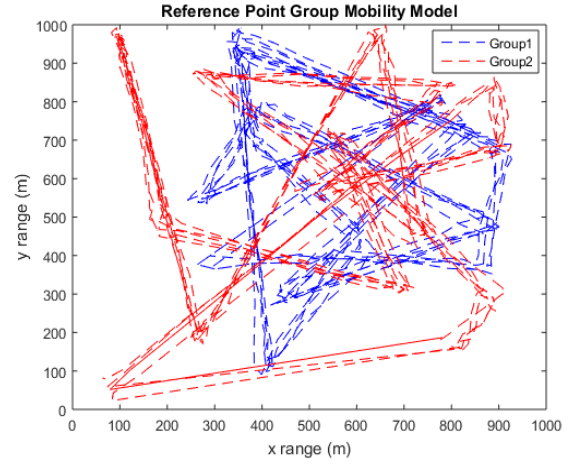


Fig. 3. RPG Mobility Model trace

The above is a description of some classic Ad Hoc mobility models, which was developed for VANETs. In recent years, with the widespread application of UAVs, its mobility model has also been developing. The Paparazzi Mobility Model [10], Particle Swarm Mobility Model and Smooth-Turn Mobility Model for FANETs have emerged.

D. Particle Swarm Mobility Model

The Particle Swarm Mobility Model [11] was designed for FANETs. The model is based on three characteristics of UAV: first, UAV nodes cannot run in a purely random manner; second, UAV should perform tasks in groups; third, collision avoidance should be considered when multiple UAVs cooperate in mission execution. The whole process of the model is divided into two stages. The first stage is to use particle swarm optimization model to generate path trajectories, and the second stage is to use collision avoidance algorithm to prevent collisions between UAV nodes. The trajectory generation equation for the first stage is given below:

$$V_i(t) = (1 - \alpha)V_i(t-1) + G \quad (6)$$

$$G = \alpha\varphi\left(\frac{gCenter(t-1) - wp_i(t-1)}{\Delta t}\right) \quad (7)$$

$$wp_i(t) = wp_i(t-1) + V_i(t)\Delta t \quad (8)$$

$$gCenter(t) = \frac{\sum_i^N wp_i(t)}{N} \quad (9)$$

where $V_i(t)$ denotes the velocity of node i at time t , $gCenter(t-1)$ denotes the global central position of node i at time $t-1$, and $wp_i(t-1)$ denotes the location of node i at time $t-1$. α is the tuning factor whose range is $[0,1]$ and by adjusting the value of α , the effect of historical speed on current speed is changed. φ is a random variable consistent with the Gauss distribution. The model takes into account both the temporal correlation on the mobility of a specific UAV itself and the spatial correlation across multiple UAVs that fly as a coordinated group.

E. Smooth-Turn Mobility Model

In [12], a new mobility model named smooth turning mobility model is proposed. In this model, the nodes randomly select a turning center and then choose a time period called walking time. In this time period, they move around the turning center until the next turning center and walking time

are selected after the end of this time period. The turning center is perpendicular to the direction of the node's speed, which ensures the smoothness of the generated trajectory. The correlative equations of the velocity and position of the model are given below:

$$a_t(t) = 0 \quad (10)$$

$$a_n(t) = \frac{V^2}{R(t)} \quad (11)$$

$$\dot{\varphi}(t) = -w(t) = -\frac{V}{R(t)} \quad (12)$$

$$\dot{p}_x(t) = v_x(t) = V \cos(\varphi(t)) \quad (13)$$

$$\dot{p}_y(t) = v_y(t) = V \sin(\varphi(t)) \quad (14)$$

where $p_x(t)$ and $p_y(t)$ are x and y coordinates. $v_x(t)$ and $v_y(t)$ represent the velocity of the node along the x and y directions. $w(t)$ represents angular velocity. $\varphi(t)$ represents the heading angle measured anti-clockwise. $\dot{p}_x(t)$, $\dot{p}_y(t)$ and $\dot{\varphi}(t)$ are the derivatives of $p_x(t)$, $p_y(t)$ and $\varphi(t)$ to t . $a_t(t)$ and $a_n(t)$ represent angular acceleration velocity and constant acceleration, respectively. V represents the heading speed and is a constant. $R(t)$ is the turning radius, where $R(t) > 0$ represents the right turn of the UAV and $R(t) < 0$ represents the left turn of the UAV. The angular velocity and turning radius remain unchanged within a time interval. The reciprocal of radius $\frac{1}{R(t)}$ is from Gauss distributed. The variance is σ^2 , and its mean value is zero. The time interval τ_i is from exponential distribution and its mean value is λ . By adjusting the values of parameters V , $\varphi(t)$ and σ^2 , various flight modes can be simulated. The trajectory of the model in two-dimensional environment is shown in the Fig 4, the node moves at a speed of 40 m/s and the turning radius is set to 25,000m. The red line in the figure represent the movement trajectories of the nodes, and the green dots represent the turning centers generated according to the Gaussian distribution during the movement. Although the model can describe the basic UAV movement characteristics, it does not take into account the maneuvering characteristics in the vertical direction. In paper [13], a 3D random mobility model is proposed based on this model.

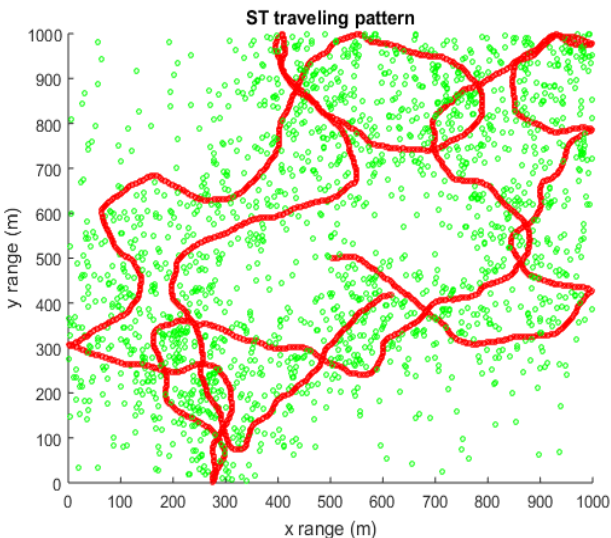
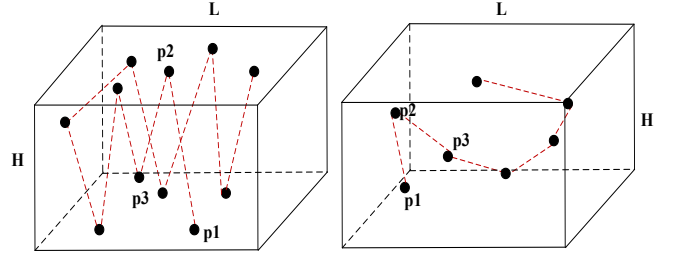


Fig. 4. ST Mobility model trace



(a) Movement without relative speed (b) Movement with relative speed

Fig. 5. The movement of a node at the same walk time

III. 3D SMOOTH RANDOM WALK MOBILITY MODEL

In this part, we extend the 2D random walk model to the 3D space according to the moving characteristics of the UAV in space. In the 2D random walk model, the nodes are initially randomly distributed in the 2D simulation area, and then the simulation node randomly chooses a speed and direction within the travel time until the end of the walk time or the arrival of the simulation boundary node. When extending random walk from 2D space to 3D space, we need to pay attention to: a) the velocity direction is three-dimensional; b) the velocity in vertical direction is relatively small after the UAV runs steadily; the velocity in horizontal direction and vertical direction are not in one scale; c) after the UAV runs steadily, it generally keeps running on the same horizontal plane, and the moving distance in vertical direction is relatively small. Because the random walk direction is generated randomly, it is necessary to smooth the generated trajectory in order to satisfy the maneuverability of UAV. After analyzing the characteristics of the UAV, the proposed three-dimensional random walk model mainly solves three problems: 3D velocity, 3D boundary processing and route smoothing. In this model, we assume that all UAV nodes are regarded as a particle, regardless of the impact of external environment such as wind and rain, and the collision between UAVs. When the UAV runs to a steady state, we assume that the altitude difference in the vertical direction is less than 100 m. The three issues mentioned above are discussed in next section.

A. Speed and Its Direction

In the two-dimensional random walk model, a speed and direction are randomly selected after the end of a walk time with the speed in a predefined range and the direction randomly selected between $[0, 2\pi]$. In the 3D smooth random walk model, we use two randomly generated directions α , β representing the angles in the horizontal and vertical directions respectively, by which a unique direction can be determined in space. The speed is still randomly generated. If the speeds in the horizontal and vertical directions are at the same scale, the UAV nodes will turn up and down frequently. The movement is shown in the Fig 5(a). In order to solve this problem, we introduce the concept of relative speed. In a 3D simulation area, the UAV is assumed to be surrounded by a square with a side length L on the horizontal plane. In the vertical direction, we assume that nodes are moving in an area with a height difference of H . During the random walk, the velocity V is randomly generated. The velocity along the X direction, the Y direction and the Z direction is calculated by the following equations:

$$V_X = V \cos(\alpha) \cos(\beta) \quad (15)$$

$$V_Y = V \cos(\alpha) \sin(\beta) \quad (16)$$

$$V_Z = V \sin(\alpha) \quad (17)$$

randomly and respectively, angles α and β are generated in vertical and horizontal directions, and the following conclusions are calculated according to the above method:

$$\overline{V}_X = \overline{V}_Y = \overline{V}_Z \quad (18)$$

where $\overline{V}_X, \overline{V}_Y, \overline{V}_Z$ respectively represent the average velocity of the node in three directions, which causes the drone node to turn to the boundary frequently in the vertical direction, as shown in the figure above. We can't simply calculate the velocity in each direction using the above method. We need to add a scale factor λ when calculating the velocity along the Z direction. The calculation method is as follows:

$$\lambda = \frac{H}{L} \quad (19)$$

$$V_Z = \lambda V \sin(\alpha) \quad (20)$$

In this way, the three-dimensional random walk ensures that the X, Y and Z directions have the same probability to reach the simulation boundary, which reduces the frequency that the UAV node turns to the upper and lower boundaries. The movement with relative speed is shown in the Fig 5(b). After adding the scale factor, the UAV nodes will rarely make such frequent turns.

B. Boundary Processing

The boundary is processed using a simple bounce mechanism in the two-dimensional random walk model. The calculated position of the next node may appear at eight locations outside the simulation area in 2D random walk. In the 3D random walk model, we use the above velocity equation to multiply the travel time to get the new node coordinates. The position of the next node may appear in one of the 26 locations outside. We use the boundary processing of the 2D random walk model and the processing method uses the bounce mechanism to process the boundary. Fig 6 is a schematic diagram of the boundary processing of the model.

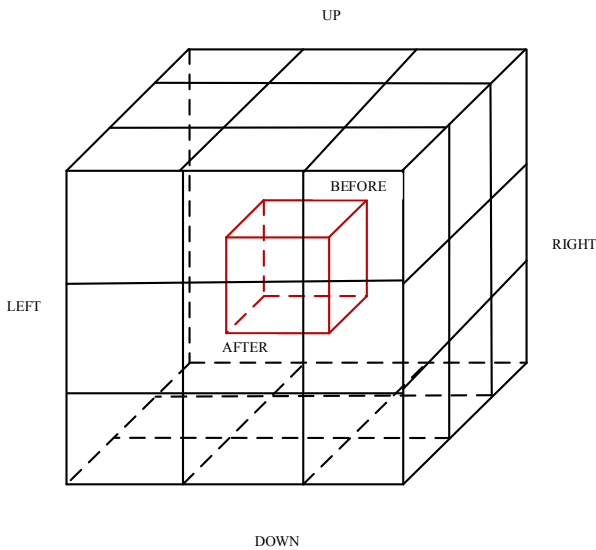


Fig. 6. The framework of 3DSRW

TABLE I. BOUNDARY PROCESSING OF 3DSRW

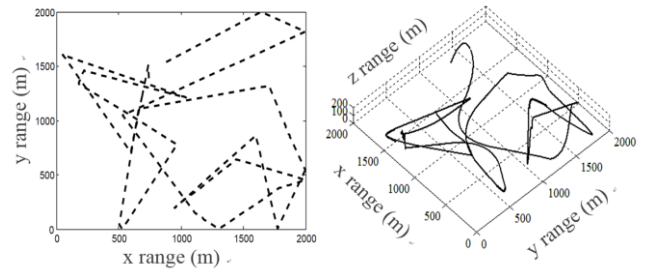
ARRIVAL BOUNDARY	VERTICAL ANGLE	HORIZONTAL ANGLE
UP	$\alpha' = 2\pi - \alpha$	$\beta' = \beta$
DOWN	$\alpha' = 2\pi - \alpha$	$\beta' = \beta$
LEFT	$\alpha' = \alpha$	$\beta' = \pi - \beta$
RIGHT	$\alpha' = \alpha$	$\beta' = \pi - \beta$
BEFORE	$\alpha' = \alpha$	$\beta' = 2\pi - \beta$
AFTER	$\alpha' = \alpha$	$\beta' = 2\pi - \beta$

The area enclosed by the red line in the figure is the simulation area. In the 3D space, the simulation boundary reached by the UAVs may be up, down, left and right, before and after. When different boundaries are reached, the reflection angles are calculated according to different calculation methods. Table 1 shows the calculation methods of reflection angle after UAV node arrives at the boundary where α and β are the incident angles in the vertical direction and the horizontal direction, respectively, and α' and β' represent the reflection angles after the node reaches the simulation boundary. According to one of the 26 aspects that the UAV node arrives and the angle conversion relationship of the above table, we can easily complete the conversion of the angle.

C. Track Smoothing

During a period of time, a UAV node reaches p3 from position p1 through p2, resulting in a sharp turn as shown in Fig 5(a). For the sharply curved trajectory generated by the three-dimensional random walk strategy, we use B-spline curve to smooth the generated trajectory and make the model more suitable. By smoothing the track on the basis of the original track, a smooth track conforming to a certain dynamic constraint is generated, so that the UAV's motion state (angular velocity, linear velocity, etc.) is continuously changed. Trajectory smoothing makes the subsequent protocol simulation more realistic, so as to obtain more accurate experimental results.

Through the above three steps, the proposed model generate a relatively smooth moving trajectory in 3D space as shown in Fig 7(b). Fig 7(a) shows the trajectory generated by the 2D random walk model at the same speed and travel time. By comparing the generated trajectories, we can see that the proposed model overcomes the unfightable situation of UAV caused by small turning angle in 2D. The movement in 3D space is more in line with the characteristics of the UAV. Next we experiment to verify the performance gap of the routing protocol in 3D space and 2D plane.



(a) random walk trace in 2D (b) the trace generated by 3DSRW

Fig. 7. The framework of 3DSRW

IV. EXPERIMENTAL DESIGN AND RESULTS ANALYSIS

In this part, we evaluate the proposed 3D Smooth Random Walk Mobility Model. First, we verify that in a real environment, setting the UAV nodes in FANETs on the same level is not in line with real flight missions. There is a big gap in the performance of various routing protocols in 3D and 2D environments. Then the 3DSRW mobility model is applied to compare the network performance metrics of the protocols in different 3D simulation scenarios. The protocols AODV, DSDV, OLSR, GPSR are applied in our experiments.

A. Simulation Platform

In this paper, we use the network simulator NS2 [14] to conduct experiments. It is a discrete event simulation tool based on real network environment. NS2 contains a large number of network simulation modules including physical layer, network layer, application layer simulation, supporting for wireless and wired. The network simulation provides the corresponding network simulation result analysis tool. Because it has developed a large number of wireless simulation protocols at the network layer, we chose it as an experimental platform, however, there are still some problems in NS2. The biggest problem is that it does not support 3D simulation. In [15], the steps of modifying NS2 to support 3D simulation at the topological level are described in detail. The modified NS2 supports both 2D and 3D simulation.

B. Simulation Settings

The simulation scene parameters are set as shown in the following table. The 3D Smooth Random Walk Mobility Model is used to generate the UAV movement trajectory. The simulation boundary is set to 2,000m*2,000m*100m. In this environment, the number of simulation nodes is set between [20, 140], and the average speed of node movement is between [10,80]m/s and the simulation time is set to 200s. For a specific three-dimensional random walk, the travel time is set to 10s. For the network simulation parameters, we make the following settings: we use the 802.11 protocol at the MAC layer. The node communication range is 500m, and the wireless propagation model we use is the Shadowing propagation model which supports propagation in 3D space; the type of traffic is CBR, and each packet size is set to 512 Bytes; the most important parameter is set to the number of CBR connections, which represents the number of connections between UAV nodes for a period of time. Most simulation experiments use a fixed number of connections, which does not realistically simulate the network. In [16], the authors prove that the PDR and average throughput are affected by the number of CBR connections. Here the number of connections are not fix setting, and we use the following calculation method to calculate the number of CBR connections:

$$CBR\ number = \frac{UAV\ number}{10} \quad (21)$$

we consider that the more the number of UAV nodes in a simulation scenario, the more communication is brought among UAVs. A CBR connection consists of at least two nodes, including the source node and the destination node, and the remaining nodes act as the forwarding node of the packet. The simulation program runs automatically by script, and the simulation results can be obtained after the simulation ends. These results include the End-To-End delay, the average throughput, and the packet delivery ratio. In order to make the

TABLE II. SIMULATION SETTINGS

Simulation Parameters	Values
Simulation Platform	NS2.35
Simulation Area	2000m*2000m*100m
Mobility Model	3D Smooth Random Walk
Channel Type	Wireless Channel
Radio-propagation model	Shadowing
MAC Layer Protocol	802.11
Type of Traffic	Constant Bit Rate (CBR)
CBR Interval	0.1 sec
Routing Protocol	AODV, DSDV, OLSR, GPSR
Simulation Duration	200 sec
Type of Traffic	512 Bytes/Package
Node Speed	10,20,30,40,50,60,70,80 (m/sec)
Node Number	20,40,60,80,100,120,140

experimental results more accurate, we set up a variety of scenarios, for each scenario we experimented 20 times, and the final result takes the mean.

C. Routing Protocols Used in Experiment

Most of the existing FANETs routing protocols are face routing, ignoring the characteristics of UAV flying in 3D, which makes its routing performance unable to reflect FANETs more realistic. In [17], Jiang and Han present a comprehensive and state-of-the-art survey on routing for UAVs. Here, we classify the routing protocols into four categories: topology-based, position-based, swarm-based and hybrid routing protocol. Then the topology-based routing protocol is further divided into two categories: proactive routing and reactive routing protocol.

The topology-based routing protocol periodically broadcast routing table entry of the node to the neighboring node. When forwarding the packet, the node queries the next hop address in the routing table according to the target node address. Topology-based routing protocol is divided into table-driven routing protocol and on-demand routing protocol. The difference between them is the routing table update mode. AODV [18] and DSDV [19] are representatives of on-demand and table-driven routing, respectively. The OLSR [20] protocol and its improved protocols are widely applied in the FANETs environment.

In position-based routing protocol, each node knows the position information of the all nodes, and determines the next forwarding node through the position information. Therefore, each node requires to configure precise GPS devices, which results in some hardware consumption. This routing protocol is very suitable for high-speed dynamic network. The representative is the GPSR [21] routing protocol.

Swarm-based routing protocols are based on some group intelligence behaviors in nature, such as bee colony routing and ant colony routing, which are inspired by bee colonies and ant colony foraging behaviors.

The hybrid routing protocol is a routing protocol that combines the above three basic routing protocols. In [16], The author proposed a hybrid improved 3D scenario-oriented routing ITSr in complex 3D urban environments of VANETs.

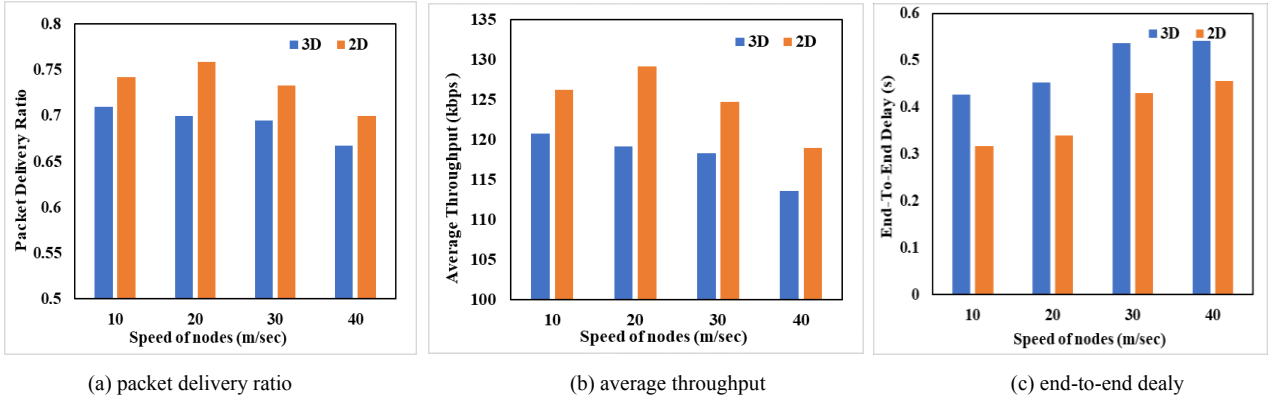


Fig. 8. Performance gaps in 2D and 3D environments of AODV

D. Performance gaps between 2D and 3D in FANETs

In this section, we verify the performance gap of AODV in FANETs in 2D and 3D space. In Fig 9, we assume that the UAV adopts an omnidirectional antenna with a wireless transmission range of R . D is the actual position of UAV in space, while D' is the projection position of UAV D on the horizontal plane. When the source node S tries to send packet to the destination node D , if the UAV nodes are flying in the same horizontal plane, the distance between the source node S and the destination node D' is $L1$. As the node D' is in the communication range of the S node, the source node and the destination node can successfully transmit packet. But in the actual 3D environment, the distance between source node S and destination node D is $L2$. Since $L2 > R$, node D is not in the communication range of node S , which leads to communication failure. In many research works, the flight characteristics of UAV in 3D environment have been neglected, leading to inaccurate experimental results.

The impact of dimensionality on performance is enormous. In order to verify this impact, we compare AODV protocol in 2D and 3D FANETs environments, respectively. The proposed 3DSRW mobility model is applied. The UAV in 3D space is projected into 2D plane to generate the same trajectory on the plane. The simulation parameter settings are shown in Table 2. Different from Table 2, we only use the simulation scenario with 40 UAV nodes, and the speed range is [10,40] m/sec. For each scenario we experiment 20 times,

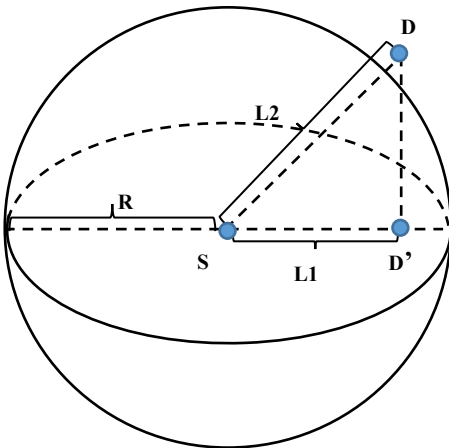


Fig. 9. Nodes in 2D and 3D environments

and the final result takes the mean. Fig 8 is the experimental results, from which we can see clearly that the performance metrics of each network in the 3D environment are not as good as those in the 2D environment. Although some achievements have been made in the research of FANETs routing protocol, most of the experiments verifying the performance of the protocol are carried out in 2D simulation scenarios, which lead to inaccurate results.

E. Result Analysis

Next, we perform a specific analysis of the performance of various routing protocols in the 3D FANETs environment, and compare the applicability of various routing protocols in 3D simulation environment.

1) AODV

In this part, we conduct a detailed analysis of the AODV protocol applied to 3D FANETs. Ad Hoc On-Demand Distance Vector (AODV) is one of the representative reactive routing protocols, which assigns dedicated time slots for packet transmission to avoid congestion and improve packet delivery ratio. In AODV, each node stores a routing table, which contains a single record for each destination and the entire network is static unless there is a need to establish a connection.

The first metric is the packet delivery ratio (PDR). The experimental results in Fig 10(a) shows that as the speed of the UAV node increases, the PDR decreases continuously. When the speed is 10m/s and 80m/s, the PDR reaches the highest value and the lowest value respectively. The density of the UAV also has a great impact on the PDR. When the number of UAV nodes is 140 and 20, the PDR reaches the lowest, and when the number of nodes is 40, the PDR reaches the highest level. Note that in the 3D FANETs environment, the AODV protocol is not suitable for dense and sparse environments. From the results obtained from various 3D simulation scenarios, AODV has excellent performance in terms of PDR. Fig 10(b) shows the performance of average throughput, where there are similar trends between Throughput and PDR. In the scenario where the UAV node is extremely sparse and dense, the End-To-End delay is large. When the number of nodes is 20 and 140, the delay reaches the highest level. When the number of nodes is 60, the delay reaches the lowest level. As the speed of the node increases, the delay increases as shown in Fig 10(c). Since the AODV protocol is an on-demand route, the network delay is a defect of the AODV protocol from the overall simulation results.

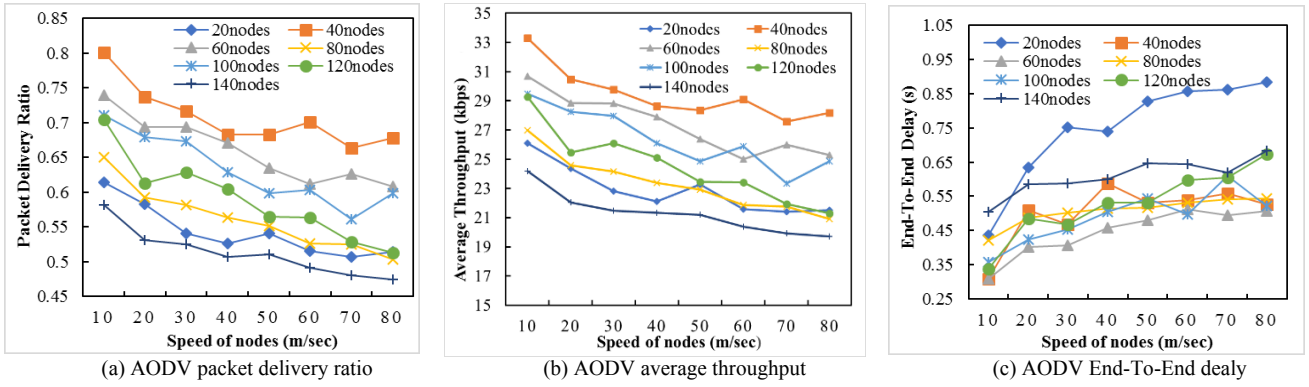


Fig. 10. AODV protocol performance analysis

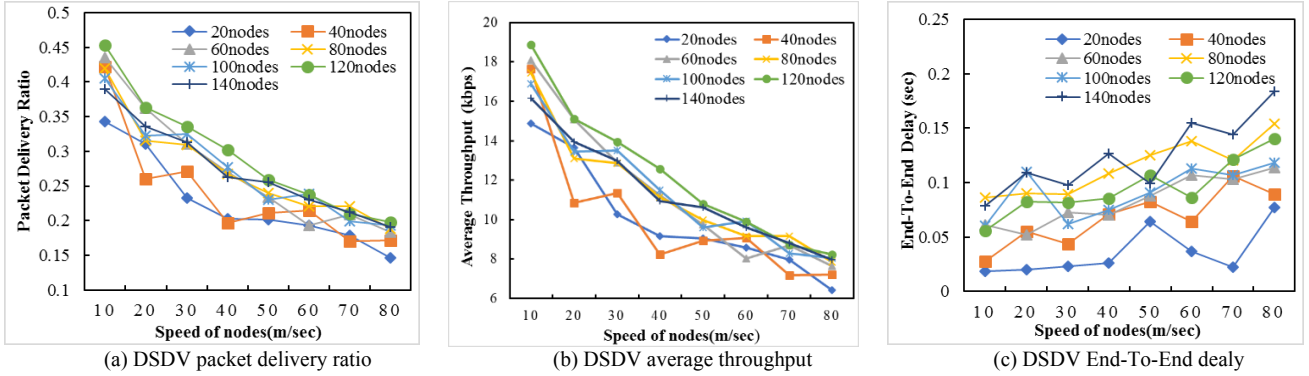


Fig. 11. DSDV protocol performance analysis

2) DSDV

In this part, we conduct a detailed analysis of the DSDV protocol applied to FANETs. Destination Sequenced Distance Vector (DSDV) is a table-driven routing protocol. In DSDV, each node keeps a route to all other nodes in a table (with sequence numbers), not just for the neighbor nodes. The table will be updated when a topology is changed. The advantage of DSDV is the use of sequence numbers to ensure loop free. Each node periodically broadcasts updates of routing table, which results in routing overhead and consumes a lot of bandwidth in the network.

The simulation results show that as the speed of the node increases, PDR and average throughput decrease continuously. When the number of UAV nodes is 120, both of them reach the highest level. The PDR and average throughput reach the lowest level when the number of nodes is 20 and 40 as is shown in Fig 11. Considering only the PDR and average throughput, the DSDV protocol is more suitable for nodes with denser interfaces in the 3D FANETs environment. Overall, DSDV has great drawbacks in PDR and average throughput in the 3D FANETs environment. As the node speed increases, the delay increases continuously as shown in Fig 11(c). When the speed of the UAV is the same, as the number of nodes in the simulation area increases, the end-to-end delay increases. Because DSDV is a table-driven routing protocol, its network delay is smaller than AODV.

3) OLSR

In this part, we conduct a detailed analysis of the OLSR protocol applied to FANETs. OLSR is improved by the traditional table-driven protocol. Each node maintains the topology information of the entire network by periodically exchanging link state information. The main idea of OLSR is each node in the network selects only a subset of its neighbor nodes as a multipoint relay set MPR. Link state information is

generated based on the nodes of the MPR. The node continuously selects its own MPR or the node make itself as the MPR. Then the node forwards the broadcast information, and finally calculates the shortest path to the destination node based on the new information. Fig 12 shows the results of OLSR routing protocol applied in 3D FANETs. The results show the PDR and average throughput has same trend as AODV and DSDV, that is, with the speed increase the PDR and average throughput decrease constantly.

The influence of UAV node density on the simulation results can not be clearly seen here. In various simulation environments where different speeds and number of nodes intersect, the velocity and node density together have an impact on the simulation results. Similar to DSDV protocol, its PDR and average throughput are lower than AODV protocol. In case of End-To-End delay as shown in Fig 12(c), as the node speed increases, the delay increases continuously. When the speed of the UAV is the same, as the number of nodes in the simulation area increases, the end-to-end delay increases. Because OLSR is a table-driven routing protocol, its network delay is smaller than AODV.

4) GPSR

Greedy Perimeter Stateless Routing (GPSR) is the first geographic routing used for UAVs. Initially, these algorithms make greedy forwarding decisions. If the packet reaches a region where progress to the destination by greedy forwarding is impossible, the algorithm enter into recovery mode by switching to face routing. Once the packet reaches a node closer to the destination than that node where greedy forwarding previously failed for that packet, the algorithm switches back to greedy forwarding again. In [14], the performance of several UAVs routing protocols, such as GPSR, OLSR, and AODV routing were evaluated. Simulation

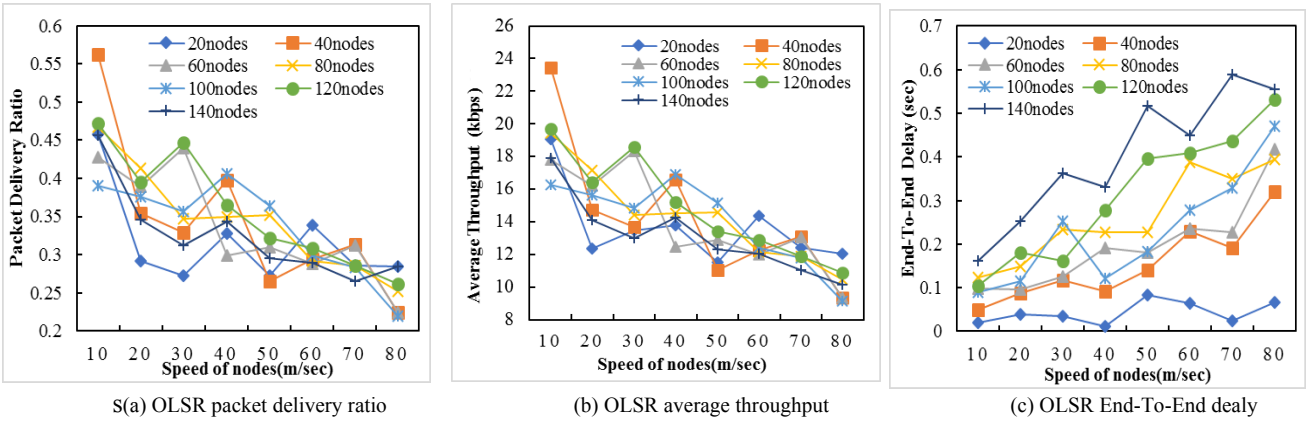


Fig. 12. OLSR protocol performance analysis

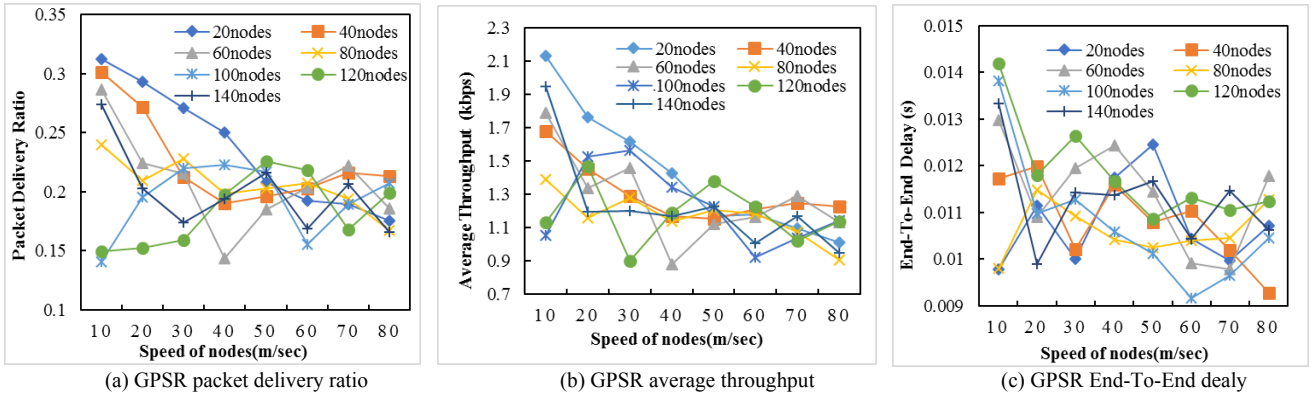


Fig. 13. GPSR protocol performance analysis

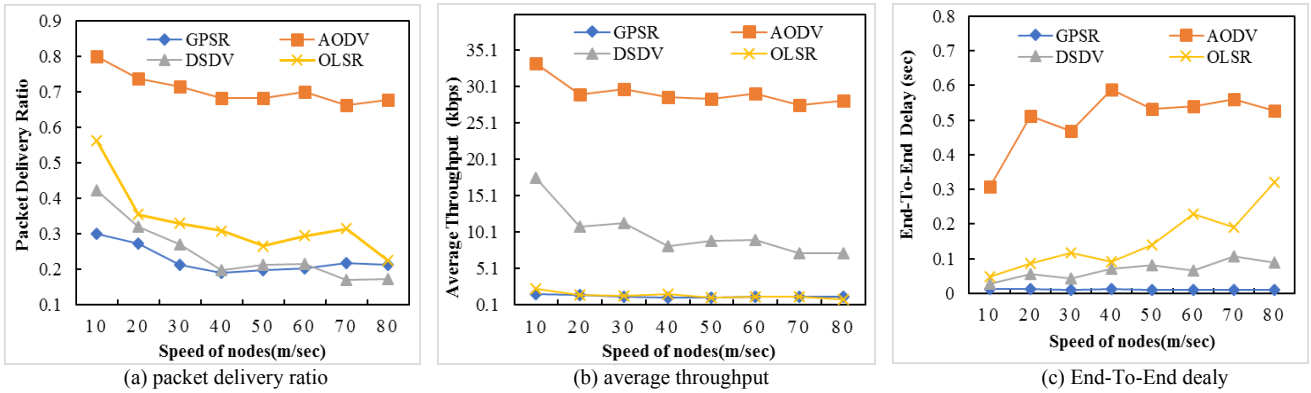


Fig. 14. Performance Comparison of Protocols

results demonstrate that GPSR outperforms AODV and OLSR with respect to packet delivery ratio and transmission delay in 2D scenarios. However, GPSR is not proper for 3D scenarios.

Compared with other protocols, the geographic location-based GPSR routing protocol is significantly better than other protocols in terms of network delay as shown in Fig 13(c), however, the protocol is applied to the 3D environment with low PDR and throughput. Any time, the node's moving speed increases, its packet delivery ratio and average throughput begin to decrease, and then remain at a lower level. Different from the other three protocols, the End-To-End delay decreases as the node moves faster.

5) Performance Comparison of Protocols

Next, we compare the selected routing protocols in the 3D FANETs environment in terms of PDR, average throughput

and End-To-End delay as shown in Fig 14. We compare the performance of different node routing protocols in the scenario where the number of nodes is 40 and here are the following experimental results. The simulation results show that the AODV protocol is superior to the other three protocols in the 3D FANETs environment in terms of packet delivery ratio and average throughput. However, the End-To-End delay of the AODV protocol is significantly higher than that of the other three protocols, which result in the protocol not suit for real-time task. In the case of the AODV protocol, it can be well applied to the 3D FANETs environment. Although the GPSR protocol has a lower delay, its packet delivery rate and average throughput are significantly lower than other routing protocols. The OLSR protocol and the DSDV protocol are not ideal for various network performances in the 3D FANETs environment.

V. CONCLUSION

With the widespread use of UAVs, research on UAVs is constantly deepening. This paper analyzes the characteristics of the UAV, and concludes that the most important feature of the UAV is to fly in 3D space. In order to further study the routing protocol of the FANETs, first we propose a 3D smooth random walk mobility model, which can mimic the movement of the UAV in 3D space. Since the NS2 simulation software does not support simulation in a 3D environment, we support 3D simulation by modifying its source code. We use the proposed mobility model to perform simulation experiments in various scenarios on various routing protocols. Experiments show that the dimension has some influence on the performance of the routing protocol. The protocol that performs well in the 2D plane is no longer the same in the 3D space. AODV protocol performs well in the 3D FANETs environment, but its network delay is inferior to the other three protocols. Next we will improve the AODV protocol based on the existing experiments.

ACKNOWLEDGMENT

This project is supported by National Science Foundation for Young Scientists of China (61701322), the Key Projects of Liaoning Provincial Department of Education Science Foundation (L201702), the Key Projects of Liaoning Natural Science Foundation (20170540700), Liaoning Natural Science Foundation (201502008, 20102175), and the Program for Liaoning Excellent Talents in University (LJQ2012011).

REFERENCES

- [1] J. Qi et al., "Search and rescue rotary-wing UAV and its application to the Lushan Ms 7.0 earthquake," *J. Field Robotics*, vol. 33, no. 3, pp. 290–321, 2016.
- [2] İ. Bekmezci, O. K. Sahingoz, and Ş. Temel, "Flying Ad-Hoc Networks (FANETs): A survey," *Ad Hoc Networks*, vol. 11, no. 3, pp. 1254–1270, 2013.
- [3] V. Sharma and R. Kumar, "G-FANET: an ambient network formation between ground and flying ad hoc networks," *Telecommun Syst*, vol. 65, no. 1, pp. 31–54, 2017.
- [4] K. Dorling, J. Heinrichs, G. G. Messier and S. Magierowski, "Vehicle Routing Problems for Drone Delivery," in *IEEE Transactions on Systems, Man, and Cybernetics: Systems*, vol. 47, no. 1, pp. 70–85, Jan. 2017.
- [5] T. Camp, J. Boleng, and V. Davies, "A survey of mobility models for ad hoc network research," *Wirel. Commun. Mob. Comput.*, vol. 2, no. 5, pp. 483–502, 2002.
- [6] J.-D. Medjo Me Biomo, T. Kunz, M. St-Hilaire, and Y. Zhou, "Unmanned Aerial ad Hoc Networks: simulation-based evaluation of entity mobility models' Impact on Routing Performance," *Aerospace*, vol. 2, no. 3, pp. 392–422, 2015.
- [7] M. Sánchez and P. Manzoni, "ANEJOS: a Java based simulator for ad hoc networks," *Future Generation Computer Systems*, vol. 17, no. 5, pp. 573–583, 2001.
- [8] B. Liang and Z. J. Haas, "Predictive distance-based mobility management for PCS networks," *IEEE INFOCOM '99. Conference on Computer Communications. Proceedings. Eighteenth Annual Joint Conference of the IEEE Computer and Communications Societies. The Future is Now (Cat. No.99CH36320)*, New York, NY, USA, 1999, pp. 1377–1384 vol.3.
- [9] X. Hong, M. Gerla, G. Pei, and C.-C. Chiang, "A group mobility model for ad hoc wireless networks," In *Proceedings of the 2nd ACM international workshop on Modeling, analysis and simulation of wireless and mobile systems - MSWiM '99*, Seattle, Washington, United States, 1999, pp. 53–60.
- [10] S. Thounhom and T. Anusas-amornkul, "The study of routing protocols for UAVs using paparazzi mobility model with different altitudes," in *Proceedings of the 2016 International Conference on Communication and Information Systems - ICCIS '16*, Bangkok, Thailand, 2016, pp. 106–111.
- [11] X. Li, T. Zhang and J. Li, "A particle swarm mobility model for Flying Ad Hoc Networks," *GLOBECOM 2017 - 2017 IEEE Global Communications Conference*, Singapore, 2017, pp. 1–6.
- [12] Y. Wan, K. Namuduri, Y. Zhou, and S. Fu, "A smooth-turn mobility model for airborne networks," *IEEE Trans. Veh. Technol.*, vol. 62, no. 7, pp. 3359–3370, 2013.
- [13] J. Xie et al., "A comprehensive 3-dimensional random mobility modeling framework for airborne networks," *IEEE Access*, vol. 6, pp. 22849–22862, 2018.
- [14] Network Simulator 2, (1995). [Online]. Available: <https://www.isi.edu/nsnam/ns/>
- [15] N. Mahmood, J. DeDoutre, and P. Pochee, "M2anet simulation in 3d in ns2," In *Proceedings of the International Conference on Advances in System Simulation, SIMUL'14*, pp 24–28, 2014.
- [16] L. Zhu, C. Li, B. Xia, Y. He, and Q. Lin, "A hybrid routing protocol for 3-D vehicular Ad Hoc Networks," *IEEE Systems Journal*, vol. 11, no. 3, pp. 1239–1248, 2017.
- [17] J. Jinfang and H. Guangjie, "Routing protocols for unmanned aerial vehicles," *IEEE Commun. Mag.*, vol. 56, no. 1, pp. 58–63, 2018.
- [18] C. E. Perkins and E. M. Royer, "Ad-hoc on-demand distance vector routing," *Proceedings WMCSA'99. Second IEEE Workshop on Mobile Computing Systems and Applications*, New Orleans, LA, USA, 1999, pp. 90–100.
- [19] C.E Perkins, P. Bhagwat "Highly dynamic destination-sequenced distance-vector routing (DSDV) for Mobile Computers," In *Proc of the ACM SIGCOMM 1994*, pp. 234–244.
- [20] T. Clausen, P. Jacquet, "Optimized link state routing protocol (OLSR)", *IETF RFC 3626*, October 2003.
- [21] B. Karp, H.T. Kung, "GPSR: greedy perimeter stateless routing for wireless networks," in *Proceedings of the 6th Annual International Conference on Mobile Computing and Networking, MobiCom '00*, ACM, New York, NY, USA, 2000, pp. 243–254.
- [22] L. Zhao, A. Al-Dubai, X. Li, G. Chen, and G. Min, "A new efficient cross-layer relay node selection model for Wireless Community Mesh Networks," *Computers & Electrical Engineering*, vol. 61, pp. 361–372, 2017.